Pergamon

Acta mater. 49 (2001) 2875–2886

Acta MATERIALIA

www.elsevier.com/locate/actamat

EVOLUTION AND MICROSTRUCTURAL CHARACTERISTICS OF DEFORMATION BANDS IN FATIGUED COPPER SINGLE CRYSTALS

Z. F. ZHANG[1, 2]†, Z. G. WANG[1] and Z. M. SUN[2]

[1]State Key Laboratory for Fatigue and Fracture of Materials, Institute of Metal Research, Chinese Academy of Sciences, Shenyang 110015, People's Republic of China and [2]AIST Tohoku, National Institute of Advanced Industrial Science and Technology, 4-2-1, Nigatake, Miyagino-ku, Sendai 983-8551, Japan

(Received 15 February 2001; received in revised form 23 May 2001; accepted 23 May 2001)

Abstract—This work investigated the dislocation arrangements, crystallographic characteristics and fatigue crack initiation of deformation bands (DBs) in a [5 12 20] copper single crystal cyclically deformed at high strain amplitude ($\gamma_{pl} = 8\times10^{-3}$). The surface morphology of the fatigued copper crystal was observed to display the following features. (1) There is only one group of fine slip bands (SBs), which seem to carry little plastic strain. (2) Intensive DBs, with a width of 50–60 μm and spacing of 100–110 μm, are homogeneously distributed on the whole surface of the crystal and perpendicular to the SBs. (3) The dislocation patterns within the SBs are often characterized by irregular structures with no persistent feature, indicating that these SBs are not typical persistent slip bands (PSBs). (4) The microstructure of the DBs can be classified into two types. One is the regular, 100% ladder-like PSBs in parallel and can be defined as the developing DB; the one is composed of parallel dislocation walls and is named the well-developed DB. (5) With further cyclic deformation, fatigue cracks always nucleate within the DBs rather than within the SBs or PSBs. Based on the observations above, the crystallographic characteristics and dislocation arrangements of DBs are discussed in combination with the plastic strain distribution and fatigue cracking mechanism within DBs. It is suggested that there is a transformation of deformation mode from slipping on the (111) plane in the developing DBs to shearing on the ($\bar{1}01$) plane in the well-developed DBs. Furthermore, the fatigue cracking within the DBs carrying high plastic strain can be attributed to the surface roughness caused by the shearing irreversibility of DBs.

Keywords: Deformation bands; Fatigue; Dislocations

1. INTRODUCTION

Fatigue crack initiation and propagation play an essential role in the failure process of metallic materials subjected to cyclic loading. To reveal the fatigue damage mechanisms of metallic materials, several workers, in past decades, have made great contributions to the microstructural evolution and damage mechanisms of fatigued crystalline materials, typically copper single crystals. There are presently a wealth of experimental data and several excellent review articles concerning different aspects of the subject [1–4]. By plotting the saturation stress τ_s versus the applied plastic strain amplitude γ_{pl}, Mughrabi [5] proposed the well-known cyclic stress–strain curve (CSSC) of copper single crystals with single-slip orientation. The most important and interesting finding in the CSSC is that there exist three well-differentiated regions defined as A, B and C at different strain range. In region A, the deformation is fairly uniform over the whole specimen with no signs of strain localization so that fatigue cracks cannot be formed, and the strain amplitude of 6.5×10^{-5} was defined as the fatigue limit of copper single crystals [6, 7]. In region B of the CSSC, the plastic strain is mainly localized in the narrow persistent slip bands (PSBs), and a two-phase (PSBs and veins) model was proposed to explain the plastic strain distribution of the specimen [8, 9]. However, to date, the dislocation structure and deformation mechanism are still a puzzle and the two-phase model will be invalid when the copper single crystals are cyclically deformed at the end of region B. For example, a very interesting question is whether it is possible for PSBs to fill the whole crystals, when the copper single crystal is just cycled at the plastic strain amplitude of 7.5×10^{-3}. As the applied strain amplitude reaches region C, the saturation stress τ_s of the copper single crystal increases again with increasing strain amplitude. This

† To whom all correspondence should be addressed.
E-mail address: zhfzhang@imr.ac.cn (Z. F. Zhang)

1359-6454/01/$20.00
PII: S1359-6454(01)00219-1

stage has been characterized by the activation of secondary slip systems and the subsequent formation of cell and labyrinth dislocation structures [1–5]. However, the deformation and damage mechanisms of the copper single crystals cyclically deformed in this region of higher plastic strain amplitudes have not been well documented so far.

Besides the well-known regular slip bands, another important deformation feature, defined as deformation bands (DBs), was frequently discovered in deformed crystalline materials [10–16]. It has been known since 1940 that a DB is a zone in which the crystal orientation differs in a distinct manner from the surroundings [10–12]. Kuhlmann-Wilsdorf [15] classified DBs into several types, such as shear bands, secondary glide bands, transition bands, kink bands and so on. These DBs can be formed under large plastic deformation, such as rolling, tensile or shearing, and often have a strong impact on the technological forming process, resulting in deformation texture and recrystallization. Recently, DBs were widely observed in fatigued copper single crystals with different orientations [17–25] and aluminum single crystals [26–30]. It was found that DBs nucleated easily when the copper single crystals were oriented for double- and multi-slip, whereas, for copper single crystals with the single-slip orientation, the formation of DBs is confined to very high strain amplitude. In contrast to PSBs, investigations on DBs are fairly rare so that the formation mechanism and microstructure of DBs are less understood. It is not very clear whether the DBs have some crystallographic habit planes with low index, and what kinds of microstructures occur within them. On the other hand, in copper single crystals, it is well known that fatigue cracks always nucleate along the surface roughness caused by PSBs at low and intermediate strain amplitudes [3, 4, 31–34]. However, because of the lack of systematic studies, the fatigue damage mechanism of copper single crystals at high strain amplitudes (up to 10^{-2}) is not very clear. It should be borne in mind that fatigue crack nucleation is primarily a surface-related effect and the disruption of an initially smooth surface by the formation of DBs will affect the process of fatigue cracking. Saletore and Taggart [17] found that the fatal fatigue crack nucleated and propagated along the macro DBs in a [122] copper single crystal. Recently, Gong *et al*. [19–21] and Li *et al*. [22–24] systematically investigated the formation of DBs in fatigued copper single crystals with double- and multi-slip orientations. But fatigue crack initiation caused by DBs was not involved. Since the deformation of crystals with double- and multi-slip orientations is often associated with the operation of secondary slip systems, the formation of DBs becomes more complicated. Therefore, in the present study, a typical single-slip oriented crystal was employed to avoid the activation of secondary slip systems, and the investigation was focused on the fatigue cracking mechanism within DBs. Meanwhile, the electron channeling contrast (ECC) technique in conventional scanning electron microscopy (SEM) has received much interest in studying dislocation arrangements in deformed materials [35–43]. This technique not only can provide a real and wide view of dislocation substructures conveniently, but also makes it possible to establish the relationship between dislocation arrangements and crystallographic characterization of the deformed crystals. In particular, the dislocation arrangements at some special sites, such as PSBs [36–38], grain boundaries (GBs) [40, 41, 43] and the front of the crack [42, 44], can be successfully revealed by this technique. Thus, in the present work, the ECC technique was utilized to examine the dislocation arrangements near fatigue cracks and within DBs over the whole surface of the crystal specimen. Furthermore, the damage mechanisms induced by DBs in the copper single crystal cyclically deformed at higher strain amplitude were also clarified.

2. EXPERIMENTAL PROCEDURE

A bulk copper single crystal was grown from oxygen free high conductivity copper of 99.999% purity by the Bridgman method. A fatigue specimen with dimensions of 8 mm×3 mm×60 mm and a gauge section of 6 mm×3 mm×16 mm was cut by an electron-spark cutting machine. The grain orientation (G) of the specimen was determined by the electron backscattering diffraction (EBSD) technique in a Cambridge S360 scanning electron microscope (SEM), with the following result:

$$G = \begin{bmatrix} 0.5929 & 0.2148 & 0.7761 \\ \overline{0.2988} & \overline{0.8362} & 0.4598 \\ 0.7478 & \overline{0.5045} & \overline{0.4316} \end{bmatrix} = \begin{bmatrix} 3 & 5 & 5 \\ \overline{2} & \overline{20} & 3 \\ 5 & \overline{12} & \overline{3} \end{bmatrix}.$$

Here, (0.2148, −0.8362, −0.5045) corresponds to the stress axis orientation of the specimen; in brief, this crystal can be referred to as [5 12 20] for comparison with previous work [25–30]. The Schmid factors (Ω) of the primary and secondary slip systems were calculated and are listed in Table 1. It can be seen that the ratio values ($Q = \Omega_S/\Omega_p$) of all of the secondary slip systems to the primary slip system are smaller than 0.9. Clearly, this crystal has the typical single-slip orientation in terms of the definition by Cheng and Laird [7].

Before fatigue testing, the specimen was electrolytically polished to produce a strain-free surface for microscopic observation. The specimen was deformed cyclically in push–pull on a Shimadzu servohydraulic testing machine under constant plastic strain control at room temperature in air. The applied plastic resolved shear strain amplitude ($\Delta\gamma_{pl}/2$) was

Table 1. Schmid factors of the primary and secondary slip systems of the present crystal

	B4(111)[$\bar{1}$01]	A3($\bar{1}$11)[101]	B5(111)[$\bar{1}$10]	C1(11$\bar{1}$)[011]
Ω_S	0.484	0.398	0.322	0.290
$Q = \Omega_S/\Omega_p$	1	0.822	0.680	0.616

equal to 8.0×10^{-3}, which is just above 7.5×10^{-3} at the upper end of the plateau region in the CSSC. A triangle wave with a frequency range of 0.1–1 Hz was used. The surface mophology of the specimen was observed at different intervals of cycling. After each observation of the surface mophology, the crystal was polished again to remove the slip traces and the activated dislocation patterns were observed by the SEM-ECC technique in the Cambridge S360 SEM. In general, the channeling contrast experiment can provide either a channeling pattern or a channeling contrast image, depending on the operating mode of the incident beam in the SEM. A channeling contrast is produced by using conventional image scanning with a back-scattered electron detector. The contrast in such an image is associated with the discontinuity in the channeling within the specimen. Any crystallographic defect that produces a distortion in the lattice, such as a twin, a subgrain or a dislocation, can be observed. Such ECC images are similar in appearance to transmission electron micrographs, albeit with a lower image resolution. To compare with the transmission electron microscopy (TEM) observation, an inverted imaging mode was adopted in the present investigation. Accordingly, the bright areas in the ECC micrograph represent the dislocation-poor regions, whereas the dark areas should correspond to the dislocation-dense regions.

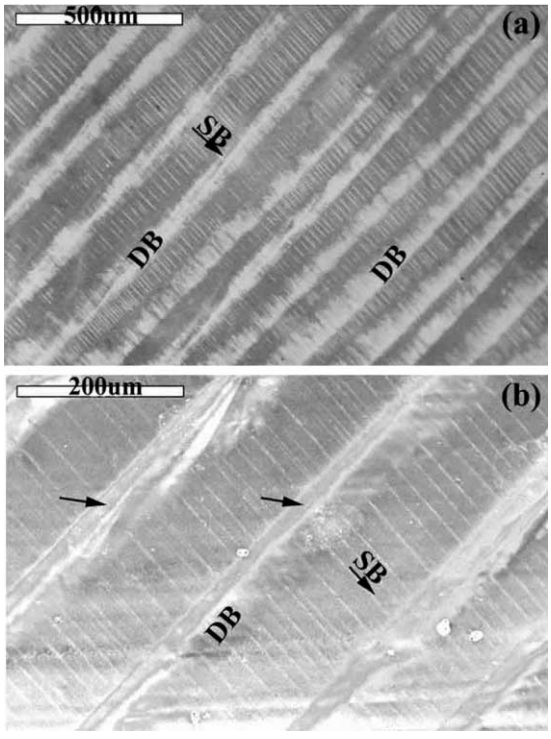

Fig. 1. Surface deformation morphology of the fatigued copper crystal.

3. EXPERIMENTAL RESULTS

3.1. Surface deformation morphology

After the single-crystal specimen was cycled at a plastic strain amplitude of $\gamma_{pl} = 8\times10^{-3}$ for 2×10^4 cycles, the surface deformation morphology was first observed by SEM. Figure 1(a) shows the deformation morphology on one of the specimen surfaces. Clearly, two striking deformation features can be seen. One is the parallel macro DBs with white contrast, which are at an angle of 45° with respect to the loading direction. It seems that these macro DBs protrude from the specimen surface. Meanwhile, the DBs are full of the dense and short slip bands. Besides the macro DBs, there is only one group of slip bands between DBs, as marked as SB, which should be the primary slip bands in the crystal. These SBs are relatively thinner and cannot penetrate into the DBs, showing a discontinuous distribution. However, DBs can spread over the whole surface and have an average width of 50–60 μm, which is about 15–20 times thicker than the SBs. DBs and SBs are roughly perpendicular to each other and the spacing of the DBs is about 100–110 μm. Except for the DBs and SBs, there are no secondary slip bands to be observed on the surface even though the applied strain amplitude is very high. Since all of the Q values of the crystal are smaller than 0.90, as listed in Table 1, the secondary slip systems might be restrained. It seems that DBs predominate the deformation of the crystal during fatigue, when the applied strain amplitude lies at the upper end of the plateau region in the CSSC. After the fatigued crystal specimen was polished to remove the existing DBs and SBs, and then cycled for 10 more cycles at the same strain amplitude, surprisingly both the DBs and SBs were activated again as shown in Fig. 1(b). But the plastic deformation within DBs was more severe than that within SBs. This indicates that DBs might carry more plastic strain than SBs during the cyclic deformation at higher strain amplitude. Especially, there seems to be a step in the middle of the DB, as indicated by the arrows in Fig. 1(b). This feature has never been reported before and might be a new finding of DBs.

3.2. Dislocation configuration within a DB

Using the SEM-ECC technique mentioned above, the polished specimen was observed to examine the dislocation arrangements within the DBs and SBs. Figure 2(a) shows the microstructure of one DB and the adjacent regions on the same surface as in Fig. 1. It can be seen that the DB has a boundary with the adjacent regions and interrupts the white SBs. The microstructure between DBs consists of SBs and irregular dislocation loop patches (veins), as shown in Fig. 2(b) and (c). The boundary between the DB and adjacent regions seems to be not distinct, indicating that the DB might be propagating towards the outside. In Fig. 2(c), several irregular SBs can be seen to terminate at the DB. Apparently, the dislocations within the SBs did not show a clear ladder-like structure as is typical in PSBs. Accordingly, the SBs could not be regarded as real PSBs with ladder-like structure. Further observations show that the DB is composed of 100% ladder-like PSBs in parallel as shown in Fig. 2(d). Hereafter, we define the DB containing 100% PSBs as the developing one and shall discuss it in the following sections.

3.3. Dislocation arrangement within different DBs

When the magnification is relatively low, several DBs can be seen in one field of view. In Fig. 3(a) there are four DBs in total, marked as 1, 2, 3 and 4, respectively. As shown in Fig. 3(a), there are some SBs between the regions of DB1 and DB2, DB3 and DB4, whereas SBs do not appear in the region between DB2 and DB3, indicating that these SBs are discontinuous on the whole specimen surface. This observation further indicates that the activated primary slip bands could not penetrate through the whole crystal specimen and did not display a persistent feature during cyclic deformation. Therefore, the SBs are different from the PSBs formed in single crystals cycled at low or medium plastic strain amplitude. If DB1 was observed at relatively higher magnification, as shown in Fig. 3(b) and (c), the dislocation arrangement was found to be full of parallel PSBs with the ladder structure, which is identical to the configuration observed in Fig. 2. In Fig. 3(b), there is a transition region (marked as T) between DB and its adjacent region with SBs. The dislocation arrangement within the transition region is irregular and obviously different from those within the center of the DB and veins. It seems that DB1 may grow into the vein region with further cyclic deformation. In addition, SBs within veins are in line with the PSBs within DB1, indicating that there may not exist a crystallographic rotation between DB1 and its neighboring regions. Whether there is a crystallographic rotation or not will be discussed in the following sections to reveal the deformation mechanism of DBs.

Apart from the dislocation arrangements in Fig. 2 and Fig. 3(b) and (c), there is another type of dislocation configuration within a DB. When DB2 in Fig. 3(a) is magnified, it is interesting to find that the dislocation arrangement consists of 100% dislocation walls in parallel [see Fig. 3(d) and (e)] and is quite

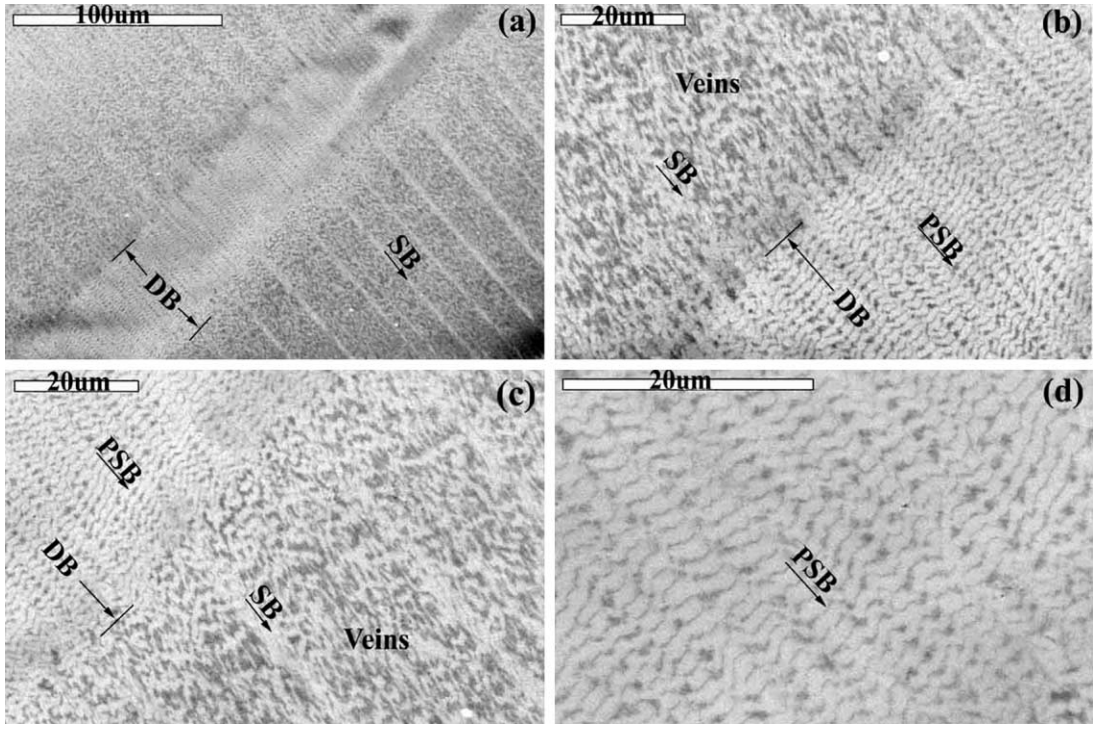

Fig. 2. Dislocation arrangements within the same DB.

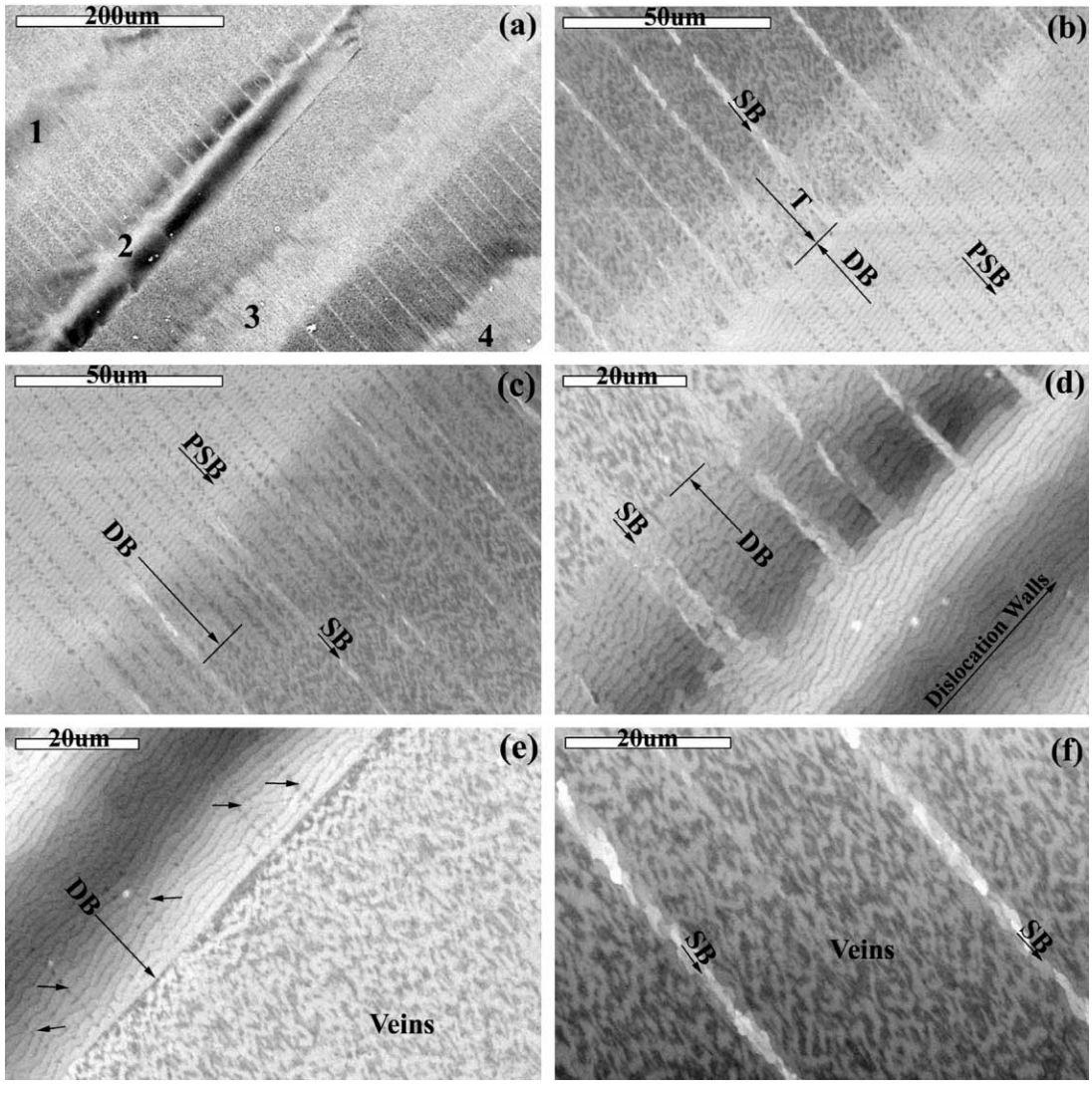

Fig. 3. Dislocation arrangements within different DBs.

different from those observed above. From one side of DB2, some SBs can penetrate into it over a certain distance [see Fig. 3(d)]. Meanwhile, within DB2, there are no ladder-like PSBs, and the dislocation walls are parallel to the DB direction. But in some local sites of DB2, some ladder traces of PSBs can be seen as indicated by arrows in Fig. 3(e), although they are not quite clear. It is suggested that the dislocation walls might evolve from the ladder-like PSBs due to the avalanche of dislocations induced by accumulation of plastic strain. In addition, as shown in Fig. 3(a), there is a bulge in the middle of DB2 and two curved bands near its boundaries. Therefore, DB2 might carry more severe plastic deformation than other DBs. Another feature of DB2 is that there is a clear boundary with the adjacent region, indicating that the propagation of DB2 might be stopped [see Fig. 3(e)]. As for the dislocation arrangement within DB3 and DB4, it was found that they are quite similar to those observed in Fig. 2 and Fig. 3(b) and (c).

When observations were focused on the regions without DBs, irregular arrangements of dislocations with higher density were found as shown in Fig. 3(f). They are quite similar to the vein structure (or matrix) in copper single crystals fatigued at low or intermediate strain amplitudes. Within these regions, some SBs transfer through the veins and link two adjacent DBs. Also, it can be clearly seen that the dislocation arrangement within SBs is quite irregular and does not display the ladder-like structure. It seems that SBs may not be the fully developed PSBs and carry little plastic strain.

3.4. Two typical dislocation arrangements within DBs

From the observations above, it can be concluded that in terms of the interior dislocation arrangement,

there are two kinds of typical DB. One is full of 100% PSBs, which can be defined as the developing type, because it can grow into neighboring regions. For example, as shown in Fig. 4(a), there exists a transition region near the boundary of the DB, and the ladder-like structure is able to pass through this boundary and becomes irregular in the vein region. It is suggested that the DB is not stable, but is propagating during cyclic deformation. Meanwhile, some SBs terminate at the boundary of the DB and show a one-to-one relationship with some PSBs in the interior of the DB, indicating that the ladder-like PSBs within the DB might evolve from the SBs. This kind of DB containing ladder-like PSBs is somewhat like the observation in a $[\bar{1}35]$ copper single crystal [22]. Another DB consists of parallel dislocation walls with no ladder-like structure, as observed in Fig. 3(d) and (e). This type of DB is quite similar to that observed in a [001] copper single crystal [20]. Figure 4(b) clearly shows such a kind of DB containing dislocation walls. It can be seen that in the left upper region of the DB there is a distinct boundary, which prevents the SBs from passing through. However, in the right lower area of the DB, there exists a transition region, within which the SBs can penetrate into the DB over a certain distance. The DB consisting of such parallel dislocation walls can be defined as the well-developed type, which is more stable in energy than the developing DB.

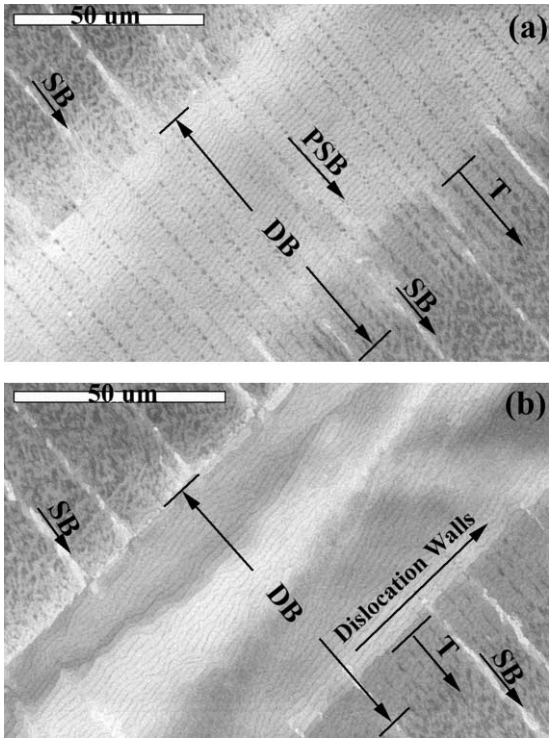

Fig. 4. Two typical dislocation arrangements within DB.

3.5. Fatigue crack initiation along DBs

When a single crystal is subjected to continuous cyclic deformation, fatigue cracks will eventually nucleate on the surface of the specimen. As can be seen clearly in Fig. 5(a), all fatigue cracks initiated within DBs rather than within the SBs. It is noted that the cracks originated mainly from the middle ridge of the DBs, as marked by arrows. To determine the preferential site for fatigue crack initiation between DBs and SBs, the whole surface of the fatigued specimen was observed by SEM. However, no fatigue cracking within SBs was observed besides some fatigue cracks nucleated within the DBs. All DB cracks are parallel to the DB direction or perpendicular to the SB direction. After the initiation of fatigue cracks within the DBs, the specimen surface was polished again to observe the dislocation structure near the cracks and further to reveal the associated cracking mechanism. As shown in Fig. 5(b), a fatigue crack originated from a DB can be clearly seen. The dislocation structure near the crack and within the DB is visible at high magnification, as shown in Fig. 5(c). In the right lower region of the DB, the dislocation consists mainly of wall structure. Near the crack in the upper region of the DB, the dislocation distribution becomes a cell structure. Additionally, there exist several fatigue cracks parallel to the DB direction in one DB, as shown in Fig. 5(d). With the help of the TEM technique, Tong and Bailon [44] observed the dislocation structure at different distances from the crack tip in fatigued copper polycrystals. With increasing distance from the crack tip, different dislocation structures such as cells, walls, PSBs, veins, loop patches and dislocation tangles could be found successively. Another finding is that the plastic deformation occurred in two or three slip systems near the fatigue crack. Recently, by using the ECC-SEM technique, Chen *et al.* [42] investigated the relationship between the dislocation cell size and the distance from the crack tip in polycrystalline copper. The result showed that the cell size increased from 0.5 to 4 μm with increasing distance from the crack tip. Also, beyond the cell structure, dense veins and PSBs, labyrinth structures and mixtures thereof were observed near the cracks. Except for copper polycrystals, the dislocation cell structure near the GBs was also observed in the vicinity of a fatigue crack in a copper tricrystal by the SEM-ECC technique [43]. All of these observations provide evidence that the dislocation cell seems to be the predominant structure near a fatigue crack no matter whether this fatigue crack was induced by GBs, DBs or other elements. This is because the dislocation cells can accommodate relatively higher plastic strain than the dislocation wall or PSB. Therefore, DBs containing cracks should carry more plastic strain than those without cracks during cyclic deformation. Meanwhile, it seems that a great change in the deformation

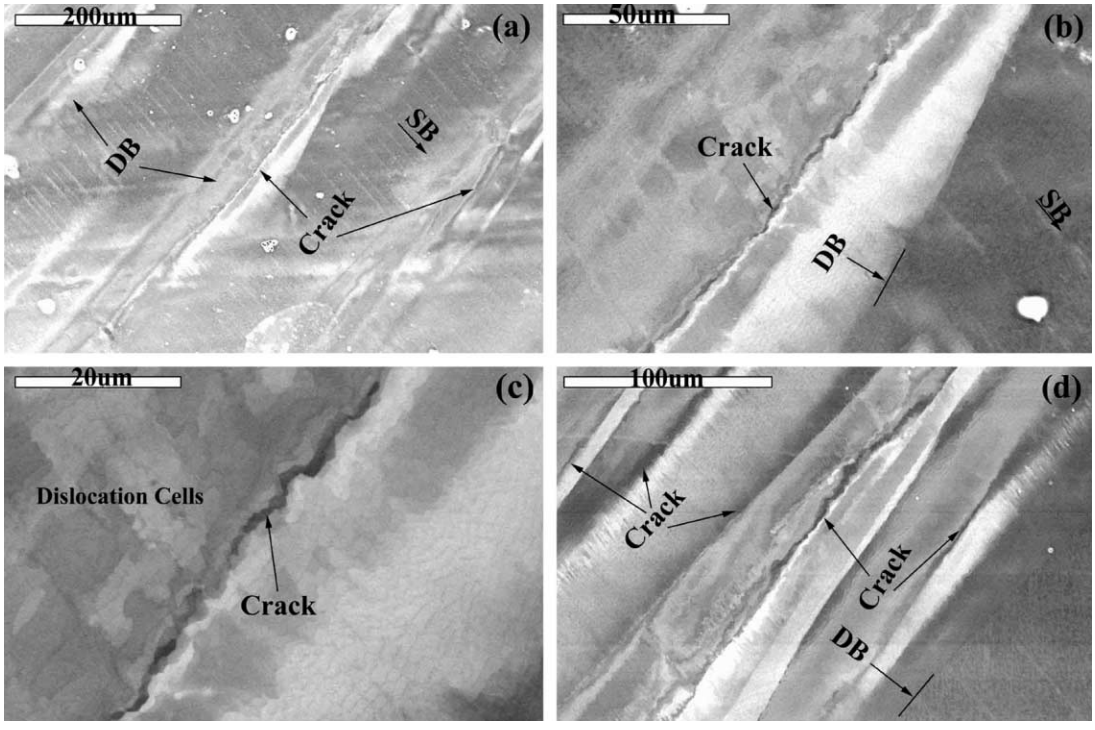

Fig. 5. Dislocation arrangements near the DBs and fatigue crack.

mode takes place for those DBs with fatigue cracks as will be discussed in Section 4.3.

4. DISCUSSION

4.1. Crystallographic characteristics of DBs

It is well known that there exist two kinds of DB, namely DBI and DBII, in cyclically deformed face-centered cubic (fcc) crystals. In general, DBI is almost parallel to the primary slip plane and DBII makes an angle with the primary slip bands. However, the formation mechanism and crystallographic characteristics of DBs have not been clearly revealed. Vorren and Ryum [26, 27] reported that DBII is parallel to the $(3\bar{1}4)$ plane for most orientations in fatigued Al single crystals, but far away from the (101) plane. In addition, a dislocation avalanche model was proposed to explain the formation of DBs during cyclic deformation [18]. A lattice rotation of about 6° between macrobands and the matrix was detected in cyclically deformed Al single crystals by using time-resolved acoustic microscopy [29, 30]. It was suggested that this lattice rotation resulted from the accumulation of the irreversible slip in one direction in PSBs and was responsible for the formation of these DBs. Recently, Gong *et al.* [19–21] and Li *et al.* [22–24] systematically investigated the formation of DBs in fatigued copper single crystals with different orientations. They found that DBI and DBII developed roughly along the primary slip plane {111} and the conventional kink plane {101} respectively, and the habit planes of DBI and DBII are strictly perpendicular to each other. They also proposed that the formation of DBI and DBII was caused by the local irreversible rotation of the crystal during symmetrical push–pull loading. However, the investigations above did not provide a clear microstructural pattern of DBs, which is of special importance to understand the formation and development of DBs.

From the relationship between DBs and SBs, it can be concluded that the present DB should belong to the DBII type. Based on the abundant dislocation observations above, it is possible to describe and reveal the crystallographic characteristics of the present DBII. A three-dimensional crystallographic picture of the ladder-like PSB is illustrated schematically in Fig. 6(a). Generally, the ladder-like structure of PSBs can be observed on the $(12\bar{1})$ plane, while parallel dislocation walls often appear on the primary slip plane (111). Clearly, these dislocation walls are perpendicular to the primary slip direction $[\bar{1}01]$. Now, let us check the microstructure of the DBs again. First, the developing DB consists of dislocation rungs of ladder-like structure [see Figs 2, 3(b) and (c), 4(a)]. Therefore, the crystallographic relationships among the primary slip plane, the developing DBII and dislocation walls can be as illustrated in Fig. 6(b). Furthermore, it is not difficult to understand why the habit plane of the DB is consistent with the dislocation rungs of ladder-like PSBs. As a result, the habit plane of the DBII should be strictly along the $(\bar{1}01)$ plane. Previously, Saletore and Taggart [17] found that, in a fatigued $[\bar{1}22]$ copper single crystal, the plane of DBII made an angle of approximately

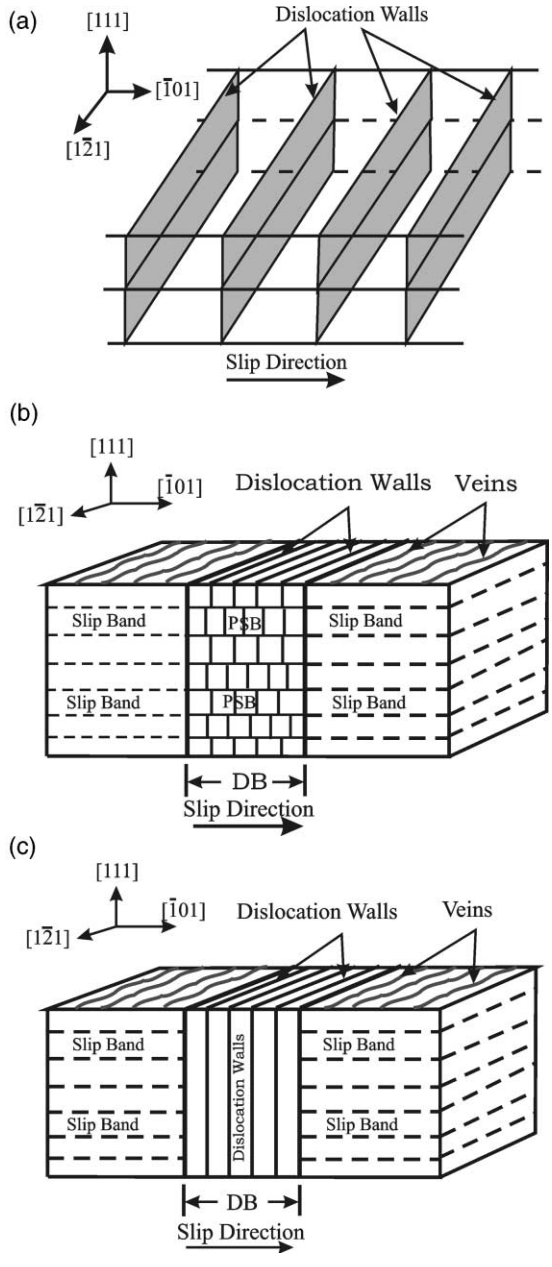

Fig. 6. Sketches of crystallographic relationships in PSBs and the present DBs: (a) PSBs with ladder-like structure; (b) the developing DB; (c) the well-developed DB.

45° to the loading direction. But they considered that the DBII was formed on the plane of maximum shear stress and did not correspond to any low-index crystallographic plane. Regrettably, the crystallographic orientation of the DB and the corresponding dislocations were not measured and observed. As we know, the interaction angle between the stress axis of a [$\bar{1}$22] single crystal and the ($\bar{1}$01) plane is just equal to 45°. Thus, it is possible for the DB to nucleate and develop along the ($\bar{1}$01) plane in the fatigued [$\bar{1}$22] copper single crystal. Secondly, for the well-developed DB, there is a transition from ladder-like structure to parallel dislocation walls [see Figs 3(d) and (e), 4(b)]. In this case, the crystallographic relationships between the primary slip plane, well-developed DBII and dislocation walls can be as illustrated in Fig. 6(c). Obviously, the well-developed DBII must have evolved from the developing one through the linking of dislocation rungs. As shown in Figs 2 and 3, the microstructure of the DB is always characterized by the ladder-like PSBs or parallel walls, which are the typical low-energy dislocations (LEDs) proposed by Laird *et al*. [2] and Kuhlmann-Wilsdorf [15]. These LEDs within the DBs may enjoy priority in the plastic strain localization and then in the initiation of fatigue cracks.

4.2. Plastic strain distribution

Since the relationship between the CSSC and the corresponding dislocation structure has been well documented in single-slip oriented copper crystals, the plastic strain distribution over the crystal is easily understood. Winter [8] and Finney and Laird [9] proposed a two-phase model for fatigued copper crystals containing vein and PSB ladder structures to explain the occurrence of a plateau region in the CSSC:

$$\gamma_{pl} = \gamma_{PSB} f_{PSB} + \gamma_M f_M, \tag{1}$$

where γ_{pl} is the applied plastic strain amplitude; γ_{PSB} is the plastic strain amplitude carried by PSBs ($= 7.5\times10^{-3}$); f_{PSB} is the volume fraction of PSBs; γ_M is the plastic strain amplitude carried by the matrix ($= 6.5\times10^{-5}$); f_M is the volume fraction of matrix. In this case, the PSBs and matrix (or veins) will appear alternately on the surface of the fatigued crystal [see Fig. 7(a)]. Since PSB is the softer phase and carries almost all of the plastic strain, the fatigue crack always nucleates within it [31–34]. However, for a copper single crystal cycled around the end of plateau region, the plastic strain distribution and the deformation mechanism are less understood. If there is no change of deformation mechanism, the fatigued crystal will be full of 100% PSBs lamellae, which can be simply illustrated in Fig. 7(b). However, instead of the occurrence of this expected deformation morphology, another deformation mode (DBs and SBs) was observed in the present work, as shown in Fig. 7(c). It indicates that the deformation mechanism of the crystal must have changed dramatically and is quite different from the two-phase model. In the present fatigued crystal, the ladder-like dislocation structures within SBs were irregular or disappeared; while DBs were full of PSBs or dislocation walls, which can be regarded as LEDs [15]. It is reasonable to suggest that DB will be much softer than the mixture of PSBs and veins and could carry almost all of the plastic strain in the present case. The surface observations in Fig. 1 provided evidence for this assumption. Therefore, the surface deformation mophology of the crystal can be as illustrated in Fig. 7(c), and the corresponding plastic strain distribution can be described as:

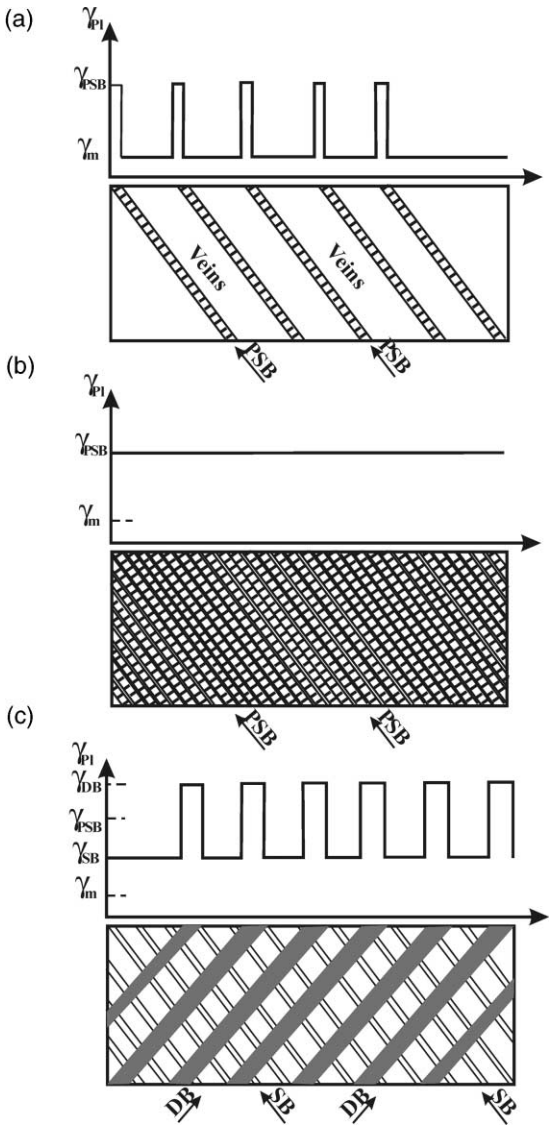

Fig. 7. Different plastic strain distributions of a fatigued copper single crystal: (a) mixture of PSBs and veins; (b) 100% PSBs; (c) mixture of DBs and SBs.

$$\gamma_{pl} = \gamma_{DB} f_{DB} + \gamma_{SB} f_{SB} + \gamma_M f_M. \quad (2)$$

Here, γ_{DB} is the plastic strain amplitude carried by DBs; f_{DB} is the volume fraction of DBs; γ_{SB} is the plastic strain amplitude carried by SBs; f_{SB} is the volume of SBs. Neglecting the effect of the matrix, equation (2) can be approximated in the following form:

$$\gamma_{pl} = \gamma_{DB} f_{DB} + \gamma_{SB} f_{SB}. \quad (3)$$

Dislocation observations revealed that the SBs did not display the typical persistent feature; as a result, the plastic strain γ_{SB} must be much smaller than the constant value of 7.5×10^{-3} owing to the hardening effect. However, DBs contain two types of dislocation structure, 100% ladder-like structure and dislocation walls, and therefore the plastic strain γ_{DB} carried by DBs must be equal to or higher than 7.5×10^{-3}. From Fig. 1, the volume fraction of DBs (f_{DB}) can be approximately calculated, which is about 0.3–0.4. As a result, the plastic strain carried by DBs will be roughly in the range of 7.5×10^{-3} to 2×10^{-2} according to equation (3). This means that a higher plastic strain amplitude is necessary for the formation of DBs. Li *et al.* [22] also observed DBs in a $[\bar{1}35]$ copper crystal fatigued at a plastic strain amplitude of 6×10^{-3}. But the formed DBs were not very strong, and their width was narrower than that of the present DBs. Obviously, with increasing strain amplitude, the DB will be stronger and can even dominate the deformation mode. It seems that there might be a critical plastic strain amplitude, γ_{DB}^{C}, for the nucleation of DBs. With increasing strain amplitude, both the width and volume of the DB will be enhanced. In the range of strain above γ_{DB}^{C}, the two-phase model will be invalid due to the formation of the DBs. Therefore, a DB can be regarded as one of the typical deformation modes in high strain fatigue.

4.3. Deformation and damage mechanism of DBs

In pure metals, it has been widely recognized that PSBs and GBs are the preferential sites for fatigue crack initiation. The GB cracking model in polycrystals has been proposed by Mughrabi *et al.* [45] and was further developed by using copper bicrystals with different GBs [46, 47]. It was proved that the impingement of PSBs against GBs plays a decisive role in intergranular cracking. As for the PSB cracking mechanism, the extrusions and intrusions on the surface were widely considered to contribute to the crack initiation. Therefore, a number of theories and mechanistic models of the surface-roughening phenomenon have been proposed to explain the PSB cracking. DBs have been recently observed in fatigued single crystals, but the fatigue damage mechanism induced by DBs received little attention. In the light of fatigue cracking in the surface roughening at PSBs, the fatigue damage mechanism induced by DBs will be discussed further below.

The slip deformation of PSBs in fcc metals is always on the (111) plane along the $[\bar{1}01]$ direction, and fatigue cracks usually nucleate along PSBs. However, the present observations discovered that fatigue cracks initiated within DBs, as shown in Fig. 5(a)–(d). Similar to PSBs, DBs can also produce surface roughening, which results in fatigue crack initiation. This result leads one to reconsider the deformation mechanism of DBs. From the dislocation pattern observed within DBs, one of the most possible deformation modes of DBs might be shearing along the habit plane of $(\bar{1}01)$, rather than slipping along the (111) plane. This special shearing deformation mechanism can be explained based on the dislocation observations and the calculation of orientation factors. As discussed in Section 4.1, it is known that the

dislocation structures within DBs are characterized by two typical arrangements: 100% PSBs or parallel dislocation walls. It is assumed that the deformation mechanism of the developing DBs within 100% PSBs still maintains the traditional mode, i.e., sliding on the (111) plane along the $[\bar{1}01]$ direction, as illustrated in Fig. 8(a). With further evolution of dislocations within the developing DBs, all of the dislocation rungs in the PSBs would be connected with each other and link up into dislocation walls gradually. Through this process, the developing DBs will be converted into the well-developed DBs by merging the ladder-like PSBs. The variation in "deformation path" has been used to discuss the bifurcation of shear banding. Zaoui *et al*. [48] pointed out that, in some circumstances, the development of internal stress is the only reason for a sudden change of the deformation path. The development of internal stress was attributed to the softening caused by the unlocking of Lomer–Cottrell barriers. It is understandable that the deformation mechanism within DBs may be changed from sliding on the (111) plane into shearing on the $(\bar{1}01)$ plane, as illustrated in Fig. 8(b). However, the shear direction on the $(\bar{1}01)$ plane in the present deformation mode is unknown. Here, we calculated some orientation factors of the shear deformation along different directions on the $(\bar{1}01)$ plane, and the results are listed in Table 2. It can be seen that there are several low-index directions with relatively high orientation factor. In particular, some orientation factors ([111], [121] directions) are equal to or higher than the Schmid factor (0.484) of the primary slip system of the single crystal. This provides some possibility of the transition of deformation from the (111) plane into the $(\bar{1}01)$ plane. Meanwhile, it is known that the well-developed DBs are full of parallel dislocation walls, which are typical LEDs. According to the hypothesis of LEDs [15], it is assumed that all the microstructures are in equilibrium with the applied stress and are, in principle, accessible to the dislocation. Since all of the developing DBs are always transformed into the well-developed ones during cyclic deformation, the occurrence of softening on the $(\bar{1}01)$ plane becomes possible. This results in the resolved shear stress on the $(\bar{1}01)$ plane being lower than that on the (111) plane when the well-developed DBs have been formed. Because of the transformation of microstructure and the decrease in the resolved shear stress, the deformation mechanism of the well-developed DBs may be changed from sliding on the (111) plane into shearing on the $(\bar{1}01)$ plane gradually. When the shearing on the $(\bar{1}01)$ plane begins to dominate the deformation of the well-developed DBs, the occurrence of fatigue cracks within the DBs will be easy to understand. As shown in Fig. 9(a), fatigue crack initiation along PSBs is due to the surface roughness induced by the slip irreversibility. Similarly, fatigue cracks can originate from the well-developed DBs by the same mechanism as simply illustrated in Fig. 9(b). In essence, the fatigue cracking mechanisms within PSBs and DBs should be identical and could be attributed to the surface roughness. The difference in fatigue cracking between PSBs and DBs is that the produced surface roughness results from the irreversibility of slipping and shearing on the (111) and the $(\bar{1}01)$ plane, respectively.

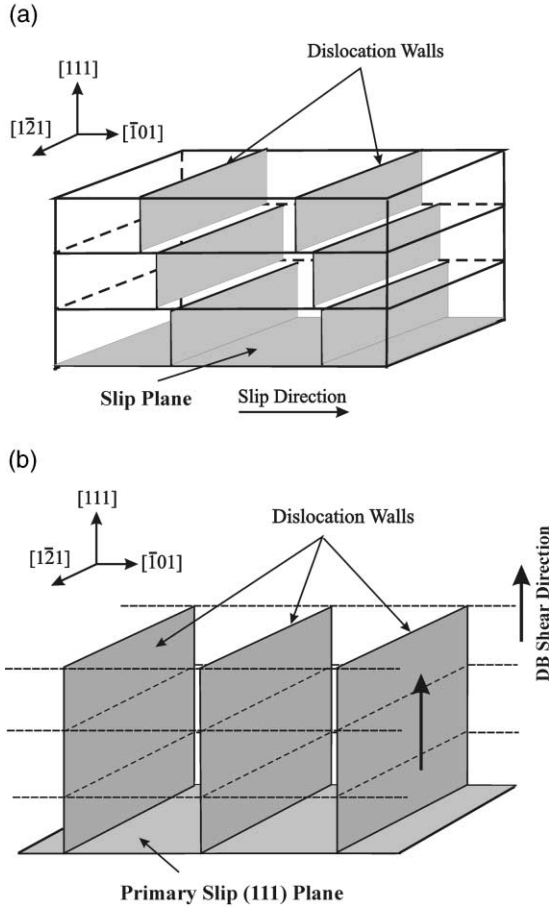

Fig. 8. Transformation of deformation modes from slipping on the (111) plane into shearing on the $(\bar{1}01)$ plane, for (a) the developing DB and (b) the well-developed DB.

Zhai *et al*. [29, 30] and Li *et al*. [24] found the occurrence of crystal rotation near the DBs, and concluded that the crystal rotation led to the formation of DBs in Al and Cu single crystals, respectively. According to the above hypothesis on the deformation mechanism of DBs, the crystal rotation took place near the DBs during cyclic deformation, but the formation of DBs was not stimulated by the crystal rotation. On the contrary, the formation of DBs induced the crystal rotation when the shearing occurred on the $(\bar{1}01)$ plane. As discussed above, the deformation and damage process of the single crystal can be understood as follows. The DBs are formed first due to the inhomogeneity of plastic strain and then, with the evolution of the dislocation pattern from the ladder-like structure into walls, the developing DBs are converted into the well-

Table 2. Possible orientation factors along different shear directions on the $(\bar{1}01)$ plane

Direction	[101]	[111]	Max	[121]	[131]	[141]	[151]
Ω_i	0.330	0.484	0.498	0.495	0.478	0.461	0.448

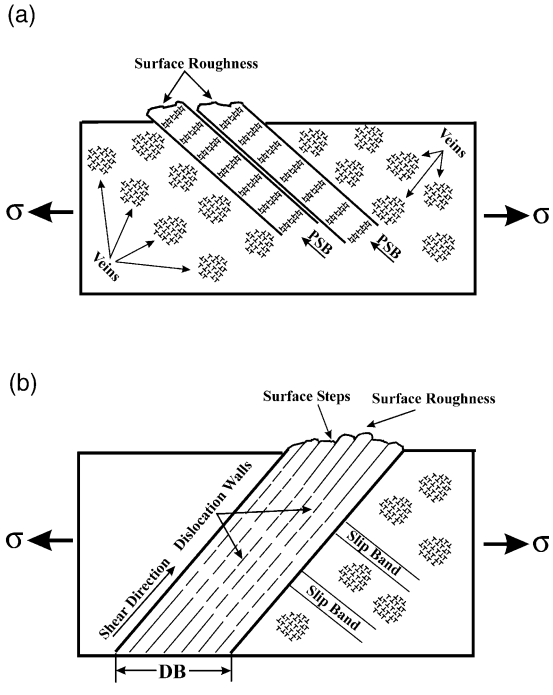

Fig. 9. Diagram of fatigue cracking induced by (a) PSBs and (b) DBs.

developed ones. Accordingly, the deformation mechanism of DBs changes from slipping on the (111) plane into shearing on the $(\bar{1}01)$ plane. With further cyclic deformation, the shear irreversibility along the $(\bar{1}01)$ plane within DBs results in the occurrence of crystal rotation and surface roughness, which finally leads to fatigue cracking within DBs.

5. CONCLUSIONS

Based on the observations and discussion above, the following conclusions can be drawn.

1. When a copper crystal oriented for single slip was cycled at a plastic strain amplitude around the end of the CSSC, two kinds of deformation feature, i.e., DBs and SBs, were formed on the whole surface of the crystal specimen. The DBs, with a width of 50–60 μm, was distributed homogeneously over the whole crystal surface, whereas the SBs did not show typical persistent features. The DB is a soft phase and carries more applied plastic strain than the SB.
2. There are two kinds of typical dislocation structure within the DBs. One is the regular ladder-like structure and can be defined as a developing DB. The other one is the regular and parallel dislocation wall structure and is called a well-developed DB. Meanwhile, the microstructures between DBs were found to be dislocation loop patches and irregular SBs. According to the crystallographic analysis and dislocation observations, it is identified that the DB observed in the present work belongs to DBII in type and has the habit plane of $(\bar{1}01)$.
3. Based on the fatigue cracking within the DBs, a new deformation mechanism of DBs was proposed. The microstructure of DBs evolves from the ladder-like PSBs into parallel dislocation walls during cyclic deformation. Correspondingly, the deformation mode within DBs changes from slipping on the (111) plane to shear on the $(\bar{1}01)$ plane, resulting in crystal rotation and surface roughness by continuous cyclic deformation. Therefore, DBs become the preferential sites of fatigue crack initiation as seen by experiment.

Acknowledgements—This work was financially supported by the Special Funding for National 100 Excellent Ph.D Thesis provided by Chinese Academy of Sciences and National Nature Science Funding of China under grant number 59971058. The authors are grateful for this support. One of the authors (Dr Z. F. Zhang) also wishes to acknowledge the Japan Science and Technology Agency (STA) for a postdoctoral fellowship.

REFERENCES

1. Kuhlmann-Wilsdorf, D. and Laird, C., *Mater. Sci. Eng.*, 1977, **27**, 137.
2. Laird, C., Charsley, P. and Mughrabi, H., *Mater. Sci. Eng.*, 1986, **81**, 433.
3. Basinski, Z. S. and Basinski, S. J., *Prog. Mater. Sci.*, 1992, **36**, 89.
4. Suresh, S., *Fatigue of Materials*, 2nd ed. Cambridge University Press, Cambridge, 1998.
5. Mughrabi, H., *Mater. Sci. Eng.*, 1978, **33**, 207.
6. Laird, C., *Mater. Sci. Eng.*, 1976, **22**, 231.
7. Cheng, A. S. and Laird, C., *Mater. Sci. Eng.*, 1981, **51**, 111.
8. Winter, A. T., *Phil. Mag. A*, 1974, **30**, 719.
9. Finney, J. M. and Laird, C., *Phil. Mag. A*, 1975, **31**, 339.
10. Barrett, C. S. and Levenson, L. H., *Trans. Metall. Soc. AIME*, 1939, **135**, 327.
11. Barrett, C. S. and Levenson, L. H., *Trans. Metall. Soc. AIME*, 1940, **137**, 112.
12. Calnan, E. A., *Acta Crystallogr.*, 1952, **5**, 557.
13. Lee, W. B. and Chan, K. C., *Acta metall. mater.*, 1991, **39**, 411.
14. Lee, C. S., Duggan, B. J. and Smallan, R. E., *Acta metall. mater.*, 1993, **41**, 2665.
15. Kuhlmann-Wilsdorf, D., *Acta mater.*, 1999, **47**, 1697.
16. Basson, F. and Driver, J. H., *Acta mater.*, 2000, **48**, 2101.
17. Saletore, M. and Taggart, R., *Mater. Sci. Eng.*, 1978, **36**, 259.
18. Li, S. X., Gong, B. and Wang, Z. G., *Scripta metall. mater.*, 1994, **31**, 1729.

19. Gong, B., Wang, Z. G. and Zhang, Y. W., *Mater. Sci. Eng. A*, 1995, **A194**, 171.
20. Gong, B., Wang, Z. R., Chen, D. L. and Wang, Z. G., *Scripta mater.*, 1997, **37**, 1605.
21. Wang, Z. R., Gong, B. and Wang, Z. G., *Acta mater.*, 1997, **45**, 1379.
22. Li, X. W., Hu, Y. M. and Wang, Z. G., *Mater. Sci. Eng. A*, 1998, **A248**, 299.
23. Li, X. W., Wang, Z. G., Li, G. Y., Wu, S. D. and Li, S. X., *Acta mater.*, 1998, **46**, 4497.
24. Li, X. W., Wang, Z. G. and Li, S. X., *Phil. Mag. A*, 2000, **80**, 1901.
25. Zhang, Z. F., Wang, Z. G. and Li, S. X., *Phil. Mag. Lett.*, 2000, **80**, 525.
26. Vorren, O. and Ryum, N., *Acta metall.*, 1987, **35**, 855.
27. Vorren, O. and Ryum, N., *Acta metall.*, 1988, **36**, 1443.
28. Zhai, T., Lin, S. and Xiao, J. M., *Acta metall. mater.*, 1990, **38**, 1687.
29. Zhai, T., Martin, J. W., Briggs, G. A. D. and Wilkinson, A. J., *Acta mater.*, 1996, **44**, 3477.
30. Zhai, T., Martin, J. W. and Briggs, G. A. D., *Acta metall. mater.*, 1995, **43**, 3813.
31. Essmann, U., Gosele, U. and Mughrabi, H., *Phil. Mag. A*, 1981, **44**, 405.
32. Hunsche, A. and Neumann, P., *Acta metall.*, 1986, **34**, 207.
33. Ma, B. T. and Laird, C., *Acta metall.*, 1989, **37**, 325.
34. Repetto, E. A. and Ortiz, M., *Acta mater.*, 1997, **45**, 2577.
35. Zauter, R., Petry, F., Bayerlein, M., Sommer, C., Christ, H. -J. and Mughrabi, H., *Phil. Mag. A*, 1992, **66**, 425.
36. Schwab, A., Bretschneider, J., Buque, C., Blochwitz, C. and Holste, C., *Phil. Mag. Lett.*, 1996, **74**, 449.
37. Ahmed, J., Wilkinson, A. J. and Roberts, S. G., *Phil. Mag. Lett.*, 1997, **76**, 237.
38. Melisova, D., Weiss, B. and Stickler, R., *Scripta mater.*, 1997, **36**, 1601.
39. Bretschneider, J., Holste, C. and Tippelt, B., *Acta mater.*, 1997, **45**, 3755.
40. Zhang, Z. F. and Wang, Z. G., *Acta mater.*, 1998, **46**, 5063.
41. Zhang, Z. F. and Wang, Z. G., *Phil. Mag. Lett.*, 2000, **80**, 149.
42. Chen, D. L., Melisova, D., Weiss, B. and Stickler, R., *Fatigue Fract. Eng. Mater. Struct.*, 1997, **20**, 1551.
43. Jia, W. P., Li, S. X., Wang, Z. G., Li, X. W. and Li, G. Y., *Acta mater.*, 1999, **47**, 2165.
44. Tong, Z. -X. and Bailon, J. -P., *Fatigue Fract. Eng. Mater. Struct.*, 1997, **20**, 1551.
45. Mughrabi, H., Wang, R., Differt, K. and Essmann, U., in *Fatigue Mechanisms: Advances in Quantitative Measurement of Physical Damage. ASTM Special Technical Publication*, Vol. 811. American Society for Testing and Materials, Philadelphia, PA, 1983, p. 5.
46. Zhang, Z. F., Wang, Z. G. and Li, S. X., *Fatigue Fract. Eng. Mater. Struct.*, 1998, **21**, 1307.
47. Zhang, Z. F. and Wang, Z. G., *Phil. Mag. Lett.*, 2000, **80**, 483.
48. Zaoui, A., Korel, A., Dubois, P. and Rey, C., *Solid State Phenom.*, 1988, **3-4**, 433.